# Flexible Aluminum Coordination in Alumino−Silicates. Structure of Zeolite H−USY and Amorphous Silica−Alumina

**Anna Omegna, Jeroen A. van Bokhoven, and Roel Prins***

*Institute for Chemical and Bioengineering, Swiss Federal Institute of Technology (ETH), 8093 Zürich, Switzerland*

*Received: January 24, 2003; In Final Form: April 30, 2003*

The aluminum coordination in amorphous silica−alumina with different aluminum concentrations as well as in pure $\gamma$-$Al_2O_3$ has been studied by means of $^{27}$Al (MQ) MAS NMR spectroscopy. The effect of ammonia adsorption at 120 °C has been studied and compared with that on zeolite H−USY, as well as with zeolites with different topologies. As for protonic zeolites, part of the octahedral aluminum reversibly changed to tetrahedrally coordinated upon ammonia adsorption on amorphous silica−alumina. The distinction between flexible aluminum coordination in zeolites and silica−alumina was possibly based on the quadrupolar parameters. Ammonia adsorption on pure $\gamma$-$Al_2O_3$ did not influence the aluminum coordination. A parallel between the structure of zeolite USY and that of amorphous silica−alumina was made on the basis of the results of $^{27}$Al MQ MAS NMR spectroscopy. A partial conversion from octahedral to tetrahedral coordination upon ammonia adsorption was observed for zeolite H−USY. Most of the flexible aluminum species belongs to an amorphous silica−alumina phase, formed during the ultrastabilization process from the reaction between the extracted silicon and aluminum.

## 1. Introduction

Ultrastable zeolite Y (USY) in its protonic form is a widely used cracking catalyst in the petroleum refining industry. It is obtained after steaming zeolite HY at high temperature and pressure.[1] During this process, aluminum atoms are removed from the framework, thus generating considerable amounts of amorphous material.[2−4] This is reflected in the $^{27}$Al MAS NMR spectrum by the presence of a signal around 0 ppm due to aluminum atoms in octahedral environment, as well as a broad component between the sharp tetrahedral signal at 60 ppm and the octahedral signal at 0 ppm. This broad resonance was assigned to pentacoordinated aluminum[5] as well as to aluminum atoms in a distorted tetrahedral environment.[6,7]

This paper focuses on the nature and the content of extraframework alumino−silicates in zeolites. Many studies have been devoted to the characterization of the extraframework aluminum species (EFAl) in zeolite H−USY.[5−12] However, the nature of these species has not been unequivocally assigned yet.

Amorphous silica−alumina (ASA) has been extensively characterized in the past decades in an attempt to correlate its structural properties with its activity in the catalytic cracking process. The aluminum atoms in amorphous silica−alumina can be tetra- or hexacoordinated.[13] It has been shown that the aluminum concentration in the synthesis mixture determines the ratio between 4- and 6-coordinated aluminum in the final material. The fraction of octahedrally coordinated aluminum increases with increasing aluminum concentration. The presence of octahedral aluminum was associated with the formation of alumina clusters.[14]

In the present work, the aluminum coordination in zeolite USY is studied as a function of treatment and a comparison with amorphous alumina and silica−alumina is made. $^{27}$Al MAS NMR spectroscopy provides information about the coordination of the aluminum species. However, the spectra resolution is reduced by the second-order quadrupolar interaction of the central transition, which shifts the position of the central transition resonance away from its isotropic chemical shift and gives broad powder patterns. Multiple quantum $^{27}$Al MAS NMR spectroscopy, developed by Frydman and Harwood,[15,16] removes the second-order quadrupolar broadening, thus allowing the detection of pure isotropic spectra. The values of the isotropic chemical shifts and quadrupolar parameters determined from the analysis of the MQ MAS NMR spectra can be used to simulate the $^{27}$Al MAS NMR spectra, leading to quantitative information on the aluminum species.[7] In this paper, we used $^{27}$Al MQ MAS NMR spectroscopy as a tool to distinguish different aluminum environments in zeolite H−USY and amorphous alumino−silicate materials. The use of a magnetic field of 600 MHz and a spinning speed of 30 kHz enabled a high resolution. The combination with quantitative $^{27}$Al MAS NMR spectroscopy provided information about the concentration of the aluminum species in the different materials.

## 2. Experimental Section

**2.1. Samples.** Table 1 reports nomenclature and description of the different samples. Zeolite USY LZ-Y84 was obtained from Linde. Silica−alumina ASA28042 and ASA26611 were provided by Shell, and $\gamma$-$Al_2O_3$ was provided by Condea. Adsorption of gaseous ammonia (10% in He) was carried out on the hydrated samples at 120 °C. After 1 h contact, the samples were allowed to cool to room temperature under ammonia flow.

**2.2. Characterization.** $^{27}$Al MAS NMR spectra were measured at 156.38 MHz on a Bruker Avance DSX-600 spectrom-

* Corresponding author. Tel: +41-1-6325490. Fax: +41-1-6321162. E-mail: prins@tech.chem.ethz.ch.

10.1021/jp030094+ CCC: $25.00 
Published on Web 08/02/2003

**TABLE 1: Nomenclature and Description of the Different Samples**

| sample | treatment | Si/Al |
|---|---|---|
| H−USY | | 2.6 |
| H−USY−$NH_3$ | 10% $NH_3$, 120 °C, 1 h | 2.6 |
| ASA28042 | | 5.2 |
| ASA28042-$NH_3$ | 10% $NH_3$, 120 °C, 1 h | 5.2 |
| ASA26611 | | 2.5 |
| ASA26611−$NH_3$ | 10% $NH_3$, 120 °C, 1 h | 2.5 |
| $\gamma$-$Al_2O_3$ | | |
| $\gamma$-$Al_2O_3$−$NH_3$ | 10% $NH_3$, 120 °C, 1 h | |

eter at a spinning rate of 30 kHz using a 2.5 mm probehead and at 104.26 MHz on a Bruker Avance AMX-400 spectrometer at a spinning rate of 12 kHz using a 4 mm probehead. The pulse length was 0.28 $\mu$s, which corresponds to $\pi/12$, for nonselective excitation.[17] The delay time was 1 s. To enable a quantitative comparison, all samples were weighed and the spectra were calibrated by measuring a known amount of $(NH_4)Al(SO_4)_2 \cdot 12H_2O$ under identical conditions.[18] For the MQ MAS NMR experiments, a three-pulse sequence, including *z*-filtering and States acquisition method, was applied.[19] The length of the first pulse was optimized in order to obtain the best efficiency for the multiquantum ($\pm$3Q) coherence creation. The second pulse was optimized to transfer the two symmetric coherences with the same efficiency into observable (−1)Q single quantum coherence. On the DSX-600 the rf field amounted to ~100 kHz for the first two pulses and to ~40 kHz for the third pulse. On the AMX-400, the rf field was ~106 kHz for the first two pulses and ~16 kHz for the third one. The relaxation delay was 0.5 s. A Fourier transform with respect to $t_1$ and $t_2$ led to pure adsorption 2D spectra. The spectra were sheared,[20] so that the orthogonal projection of the 2D spectrum on the isotropic axis gives the high-resolution 1D spectrum free of any anisotropic broadening. If the quadrupolar interaction is very small, the 2D resonance will appear as a narrow peak positioned on the diagonal ($\delta_{iso} \cong \delta_{F2}$). If the aluminum species is affected by a quadrupolar interaction, the center of gravity of the resonance shifts by the quadrupolar-induced shift. From the coordinates of the center of gravity of the different resonances, the quadrupolar coupling constants ($C_{QCC}$) as well as the isotropic

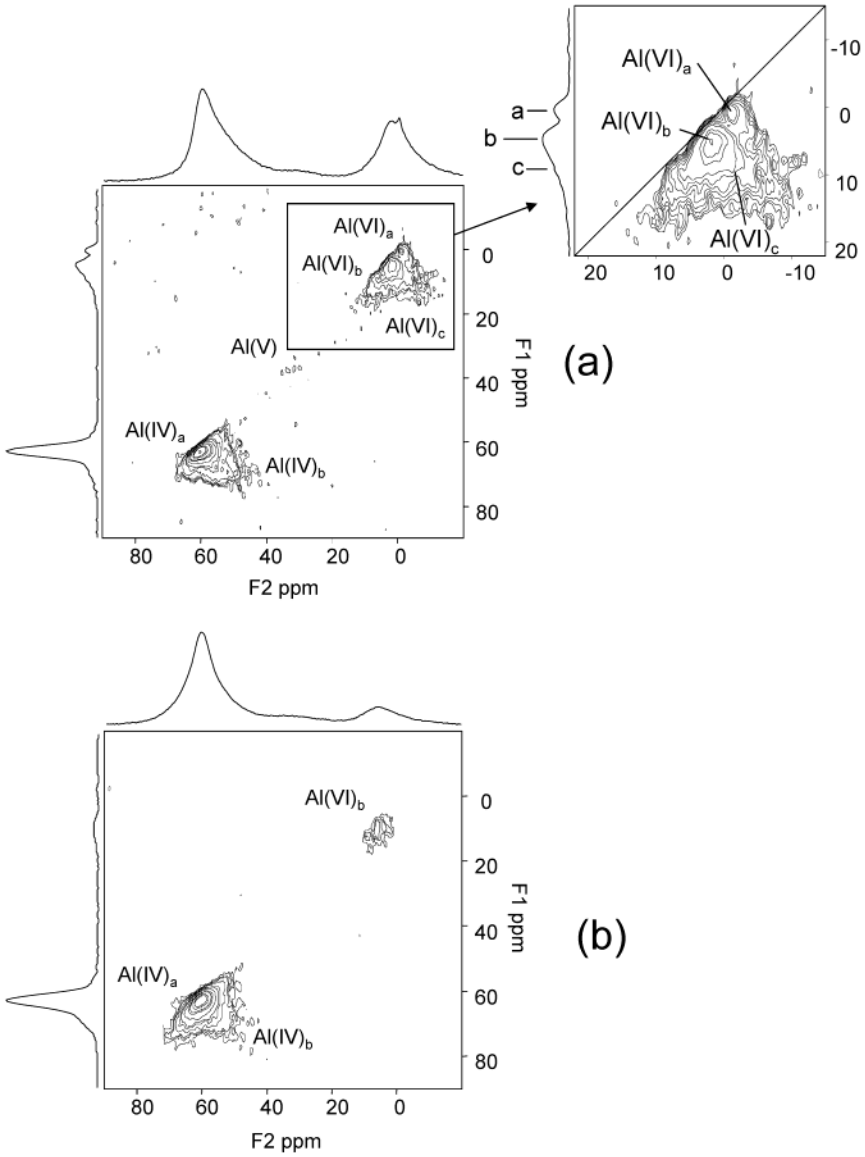


**Figure 1.** $^{27}$Al MQ MAS NMR spectra of (a) H−USY and (b) H−USY−$NH_3$ recorded at 156.42 kHz using a spinning rate of 30 kHz. The spectra are presented as a contour plot. The top spectrum is the 1D $^{27}$Al MAS NMR spectrum. The projection along the $F_1$ axis is the isotropic spectrum free of any anisotropic quadrupolar broadening. The inset shows a magnification of the octahedral region.

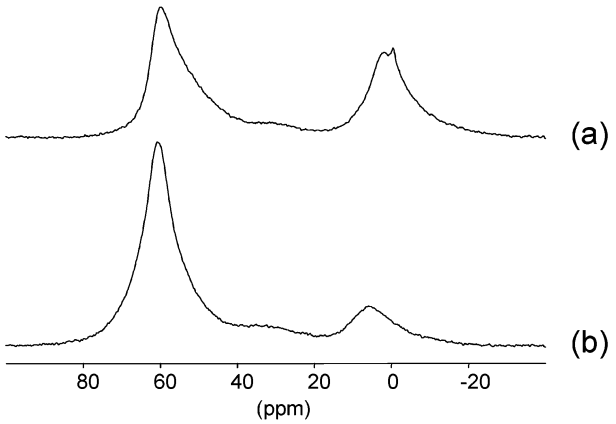


**Figure 2.** Comparison between the $^{27}$Al MAS NMR spectra of (a) H−USY and (b) H−USY−$NH_3$ taken at 156.42 kHz at a spin rate of 30 kHz. The spectra are quantitatively presented.

chemical shifts can be calculated according to the following equations:

$$\delta_{iso} = \frac{17\delta_{F1} + 10\delta_{F2}}{27} \quad (1)$$

$$P_Q = C_{QCC}\sqrt{1 + \frac{\eta^2}{3}} = \left(\frac{17}{162000}\nu_L{}^2(\delta_{F1} - \delta_{F2})\right)^{1/2} \quad (2)$$

where $\nu_L$ is the Larmor frequency. MQ MAS NMR is not quantitative, since excitation and conversion depend on the ratio $\nu_Q/\nu_{rf}$.[17] Therefore the quantification was done by fitting the corresponding 1D MAS spectra using the quadrupolar parameters determined in the MQ MAS experiment.[7]

### 3. Results

The $^{27}$Al MQ MAS NMR spectrum of zeolite H−USY is reported in Figure 1a. The spectra are presented sheared and the $^{27}$Al MAS NMR spectra of the same samples are given on top of the MQ MAS plot. The projection of the 2D frequency domain along the $\delta_{F1}$ axis gives the purely isotropic spectrum, free of second-order quadrupolar broadening. The spectrum is similar to that previously reported on the same sample.[7] At least two different contributions are distinguished in the 50−60 ppm region, attributed to tetrahedrally coordinated aluminum species, called $Al(IV)_a$ and $Al(IV)_b$, in agreement with ref 7. The peak $Al(IV)_a$ resonates close to the diagonal, indicating that the corresponding aluminum species experience a small quadrupolar interaction. Peak $Al(IV)_b$ deviates from the diagonal, indicating a large anisotropic quadrupolar-induced shift and broadening. In the octahedral region at least two resonances can be resolved in the 1D spectrum of zeolite H−USY, a narrow one and a large one. In the 2D spectrum, at least three resonances can be distinguished, $Al(VI)_a$, $Al(VI)_b$, and $Al(VI)_c$. This separation is made possible by the combination of high magnetic field and high spinning rate. $Al(VI)_a$ resonates close to the diagonal and corresponds to the narrow peak that is seen in the 1D spectrum. This peak represents only a small fraction of the total spectral intensity. The aluminum species attributed to $Al(VI)_b$ experience a relatively small quadrupolar interaction, whereas $Al(VI)_c$ shows strong quadrupolar broadening. A signal at 35 ppm of low intensity is detected, which is attributed to pentacoordinated aluminum. Figure 1b shows the $^{27}$Al MAS and the $^{27}$Al MQ MAS NMR spectra of zeolite H−USY after saturation with gaseous ammonia. In Figure 2 a quantitative comparison of the $^{27}$Al MAS NMR spectra of zeolites H−USY before and after ammonia adsorption is shown. They were simulated using the quadrupolar parameters obtained from the MQ MAS experiment. The relative amounts of the different aluminum species in H−USY and H−USY−$NH_3$ are reported in Table 2 together with the values of $\delta_{iso}$ and average $C_{QCC}$. The resonances corresponding to the octahedral species $Al(VI)_a$ and $Al(VI)_c$ disappeared after ammonia adsorption. No signal in the region of pentacoordinated aluminum is visible in the MQ MAS spectrum of USY−$NH_3$. At the same time, the intensity of both tetrahedral species increased. The overall spectrum intensity did not change, indicating a transformation of the octahedral species $Al(VI)_a$ and $Al(VI)_c$ to tetrahedral. The pentacoordinated aluminum species Al(V) probably also changed into tetrahedral, so that the total effect of ammonia adsorption is to generate aluminum species with lower coordination.

**TABLE 2: NMR Parameters, Environment, and Concentration of the Different Al Coordinations in the H−USY Samples**

| | $\delta_{iso}$ (ppm) | av. $C_{QCC}$ (MHz) | H−USY (%) | H−USY−$NH_3$ (%) |
|---|---|---|---|---|
| $Al(IV)_a$ | 61.3 | 2.3 | 25 | 27 |
| $Al(IV)_b$ | 63.7 | 6.6 | 31 | 56 |
| Al(V) | 35 | 3.2 | 5 | |
| $Al(VI)_a$ | 0 | 2.0 | 2 | |
| $Al(VI)_b$ | 2 | 2.6 | 20 | 17 |
| $Al(VI)_c$ | 4.5 | 3.7 | 17 | |

The $^{27}$Al MQ MAS NMR spectrum of ASA28042 is shown in Figure 3a. The spectral region of 50−70 ppm consists of at least two resonances corresponding to tetrahedral aluminum. Both signals show a large distribution in isotropic chemical shifts as well as $C_{QCC}$ and therefore they are not well resolved. This reflects the topological distribution of aluminum atoms in the disordered amorphous silica−alumina sample. In crystalline materials, like zeolites, the bond angles are well defined, leading to a smaller distribution in NMR parameters. The region around 0 ppm consists of a signal, due to aluminum in octahedral environment. The spread in $F_1$ and $F_2$ indicates a large distribution in isotropic chemical shift and quadrupolar interaction. The $^{27}$Al MQ MAS NMR spectrum of ASA28042 after ammonia adsorption is shown in Figure 3b. As for zeolite H−USY, most of the octahedrally coordinated aluminum species changed to tetrahedrally coordinated. Figure 4 shows the effect of ammonia adsorption onto silica−alumina samples with different aluminum content. Comparing the $^{27}$Al MAS NMR spectra of ASA28042 (spectrum a) and ASA26611 (spectrum c), it can be seen that the fraction of octahedrally coordinated species is higher when the aluminum concentration is higher. Ammonia adsorption on ASA28042 and ASA26611 gave the spectra of Figures 4b and 4d, respectively. In both silica−alumina samples, the octahedral aluminum sites changed their coordination to tetrahedral. However, the extent of the conversion was higher for the silica−alumina sample with lower aluminum loading (Table 3). Of the total aluminum amount in ASA28042 and ASA26611, 31% and 14%, respectively, changed coordination. The remaining octahedrally coordinated aluminum species account for 7% and 41% of the intensity of ASA28042 and ASA26611, respectively. For comparison, ammonia adsorption was carried out on pure alumina. The spectrum of $\gamma$-$Al_2O_3$ (Figure 5a) shows the presence of both octahedral and tetrahedral species. Figure 5b shows that adsorption of ammonia onto $\gamma$-$Al_2O_3$ does not affect the aluminum coordination.

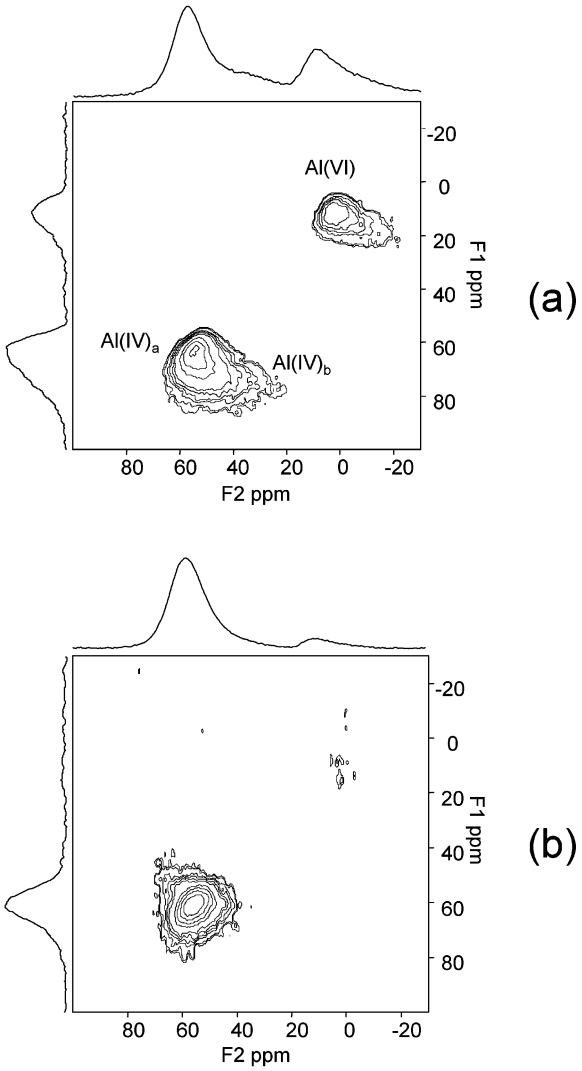


**Figure 3.** $^{27}$Al MQ MAS spectra of (a) ASA28042 and (b) ASA28042-$NH_3$ recorded at 104.26 kHz using a spinning rate of 12 kHz. The spectra are presented as a contour plot. The top spectrum is the 1D $^{27}$Al MAS NMR spectrum. The projection along the $F_1$ axis is the isotropic spectrum free of any anisotropic quadrupolar broadening.

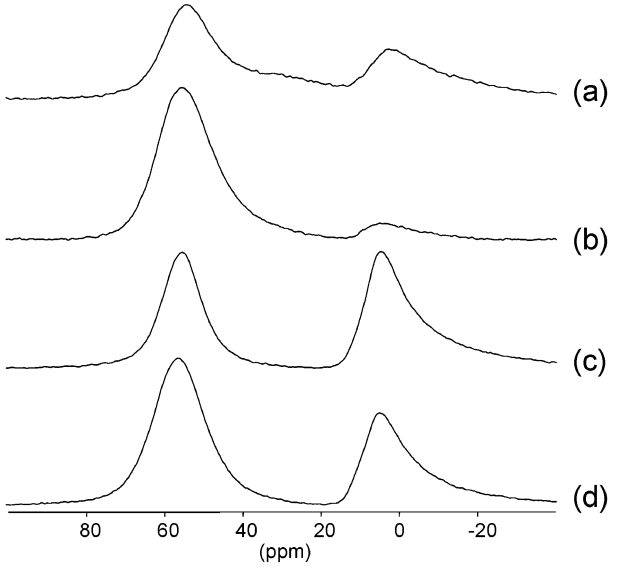


**Figure 4.** $^{27}$Al MAS NMR spectra of (a) ASA28042, (b) ASA28042-$NH_3$, (c) ASA 26611, and (d) ASA 26611-$NH_3$ recorded at 104.26 kHz at a spin rate of 12 kHz. The spectra are quantitatively compared.

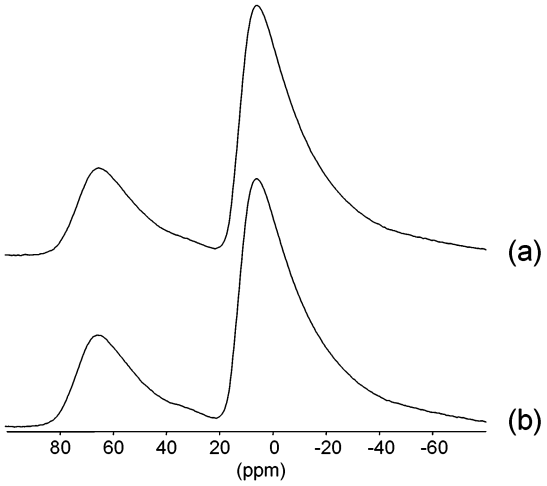


**Figure 5.** $^{27}$Al MAS NMR spectra of (a) $\gamma$-$Al_2O_3$ and (b) $\gamma$-$Al_2O_3$−$NH_3$ recorded at 104.26 kHz using a spinning rate of 12 kHz. The spectra are quantitatively compared.

## 4. Discussion

**4.1. Reversible Coordination of Aluminum Species in Alumino−Silicate Frameworks.** The presence of species with reversible aluminum coordination seems to be a general property of hydrated protonic zeolites. This phenomenon was observed for the first time by Bourgeat-Lami et al. for protonic zeolite beta.[21] They showed that the adsorption of basic molecules such as ammonia and pyridine, as well as the substitution of the protons by sodium and potassium cations, led to the recovery of the tetrahedral coordination at the expense of the octahedral coordination. From these results they concluded that the octahedral aluminum is an inherent part of the framework and that its formation is due to a distortion caused by the high electron affinity of the proton. Recently, in a MQ MAS NMR study of zeolite beta ,it was found that only aluminum atoms on specific crystalline sites are involved in the reversible tetrahedral−octahedral aluminum transformation.[22] Following the idea of Bougeat-Lami et al. they reported that Brønsted acid sites would attract water molecules to stabilize the strong electric field induced by the proton. Wouters et al. showed by $^1$H spin−echo editing MAS NMR the presence of Al−OH groups in zeolite $NH_4Y$ calcined under mild conditions.[23] They were correlated to framework-related Al−OH groups, formed upon partial hydrolysis of the lattice. The presence of aluminum species that reversibly convert their symmetry upon ammonia adsorption was also observed by Woolery et al. in zeolite HZSM-5.[24] The change in the aluminum coordination was

**TABLE 3: NMR Parameters, Environment, and Concentration of the Different Al Coordinations in the Different ASA Samples**

| species | $\delta_{iso}$ (ppm) ± 1 | $C_{QCC}$ (MHz) ± 0.5 | ASA28042 (%) | ASA28042−$NH_3$ (%) | ASA26611 (%) | ASA26611−$NH_3$ (%) |
|---|---|---|---|---|---|---|
| $Al(IV)_a$ | 61.3 | 2.9 | 40 | 49 | 45 | 59 |
| $Al(IV)_b$ | 55.0 | 4.6 | 22 | 43 | | |
| Al(VI) | 3.8 | 3.8 | 38 | 7 | 55 | 41 |

**TABLE 4: NMR Parameters and Concentration of the Octahedral Al Sites in Different Alumino−Silicate Materials**

| | H-beta | H−Y | H−mor | H−ZSM5 | ASA 28042 | ASA 26611 |
|---|---|---|---|---|---|---|
| $C_{QCC}$ (MHz) | 1.6 | 1.8 | 2.0 | 1.5 | 3.8 | 3.8 |
| total octahedral Al content (%) | 24 | 15 | 16 | 5 | 38 | 55 |
| total octahedral Al that converts upon $NH_3$ adsorption (%) | 100 | 100 | 100 | 100 | 82 | 26 |

observed not only upon treatment with a base, but also upon thermal treatment. The octahedral aluminum in both zeolites H-beta and H−Y was reverted to tetrahedral at 120 °C, indicating a low stability of the 6-coordinated framework aluminum species.[25] The structure of the zeolitic octahedral reversible aluminum species is essentially unknown. They have been tentatively described as distorted framework aluminum linked to four oxygens of the framework, the oxygen of a hydronium ion, and the oxygen of a water molecule.[21,22] Alternatively, they have been associated with aluminum species that coordinate water molecules upon partial hydrolysis of the framework.[23,24] On the basis of our results and literature reports, a tentative scheme for the process of change of the aluminum coordination in zeolites is presented below.

The reversible aluminum coordination is not a unique property of zeolites. A change in coordination as a function of the chemical environment was also observed on mesoporous Al−MCM-41 materials.[26] Our results for amorphous silica−alumina (Figures 3 and 4) show a similar change in the aluminum coordination upon ammonia adsorption. This means that this phenomenon is not an exclusive property of zeolitic framework species, but that it is a general feature of alumino−silicate frameworks. In other words, the reversibility of the aluminum coordination in zeolitic materials is not a proof for the presence of zeolitic framework octahedral species. It seems that the formation of reversible aluminum species in zeolites is associated with coordination of water molecules upon partial hydrolysis of the framework. Under these conditions, the framework will locally loose its rigidity, and the aluminum atoms will host water molecules to form framework octahedral aluminum. A similar picture for the reversible aluminum species in amorphous silica−alumina can be envisaged. In fact, due to the highly defective structure of silica−alumina, the formation of reversible aluminum species must be easier. The question arises, whether there is any difference between reversible octahedral sites in zeolites and in amorphous silica−alumina. The $C_{QCC}$ values, the relative amounts, and the percentage of conversion after ammonia adsorption for some zeolite topologies and for silica−alumina are compared in Table 4. The 6-coordinated species in acidic zeolites is affected by a small quadrupolar interaction, whereas in silica−alumina the $C_{QCC}$ average values are much higher. That means, that in zeolites this species is always characterized by a narrow line. Moreover, the relative intensities of the octahedral $^{27}$Al MAS NMR signal are low for crystalline zeolitic materials compared to amorphous silica−alumina. It is worthwhile noticing that, among the different zeolite topologies reported in Table 4, zeolite beta shows the highest relative amount of octahedrally coordinated species. This indicates that there is a similarity between zeolite beta and amorphous silica−alumina, which might be related to the high concentration of defect sites. Another difference between zeolites and silica−alumina is the extent of conversion after ammonia adsorption. The conversion is complete in the case of the zeolitic materials, whereas it is only partial in the case of the amorphous silica−aluminas.

In zeolites, framework tetrahedral aluminum is associated with Brønsted acid sites. These species are associated with an FTIR band at 3650−3550 cm$^{-1}$. Unlike zeolites, the FTIR spectrum of a dehydrated amorphous silica−alumina shows a single feature at 3745 cm$^{-1}$ in the hydroxyl region, due to terminal Si−OH groups. No band around 3600 cm$^{-1}$ due to bridged hydroxyls is observed. However, dosing ammonia onto dehydrated silica−alumina creates $NH_4^+$ species.[27] It has been proposed that apparent acid sites are produced by the interaction between the ammonia adsorbed on a Lewis acid site and a nearby surface hydroxyl group. The formation of $pyH^+$ species was also observed when pyridine was chemisorbed on dehydrated silica−alumina.[28] Similarly, the Brønsted acidity of the terminal Si−OH groups was explained by the presence of coordinatively unsaturated aluminum cations in the vicinity. This picture is compatible with our $^{27}$Al NMR results, if we assume that, in the hydrated sample, the aluminum in the vicinity of the Si−OH groups coordinates water molecules assuming an octahedral coordination. Upon dehydration and subsequent ammonia adsorption,the proton is transferred to the base, and the aluminum bridges to the oxygen of the $SiO^-$ group, thus changing its coordination from octahedral to tetrahedral.

$^{27}$Al MAS NMR spectra of silica−alumina before and after ammonia adsorption showed a partial conversion of 6-coordinated aluminum to 4-coordinated. A comparison between spectra of Figures 4b and 4d indicate that the amount of reversible aluminum species is an inverse function of the aluminum concentration (Table 3). In contrast, in $\gamma$-$Al_2O_3$ the aluminum coordination was not affected by saturation with ammonia vapor. This suggests that at least two types of octahedral aluminum are present in silica−alumina. A fraction of 6-coordinated species represents aluminum atoms that are able to convert their coordination upon ammonia adsorption, as discussed in the previous paragraph. The second fraction of species probably represents alumina domains in silica−alumina. The formation of these domains results from the difficulty of dispersing aluminum in the silica matrix, and is favored for silica−alumina with high aluminum content.

**4.2. Scheme for the Reversibility of the Aluminum Coordination.** On the basis of results of the present work and literature reports, the following scheme is proposed for the evolution of the aluminum coordination in zeolites. It is taken into account that the aluminum coordination is a function of the exact conditions in which samples are measured.

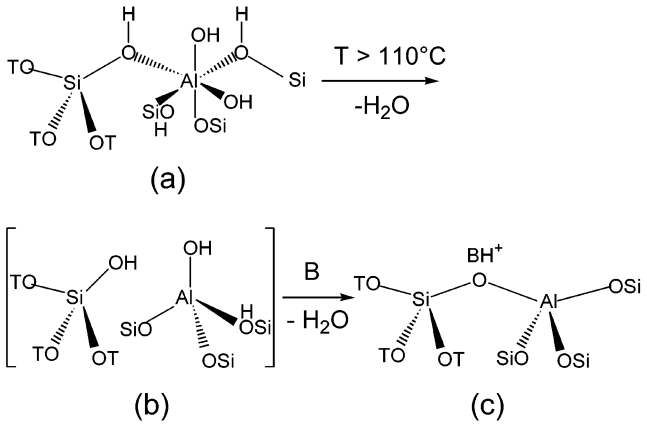

In wet conditions, species (a) is formed, in which the aluminum is octahedrally coordinated according to the $^{27}$Al MAS NMR and Al K edge XANES results.[25] This model deviates from that proposed by Bourgeat-Lami et al., in which the aluminum is thought to be connected to the framework via four oxygen atoms, to one water molecule, and one hydronium ion.[21] Because Si has a lower electronegativity than H, the Al−O−Si bridging oxygen is more negative than the oxygen in Al−OH. Species (a) is therefore more likely to exist. The model (a) does not take into account additionally hydrogen-bonded water molecules forming a hydration sphere around the site. Species (b) corresponds to the tetracoordinated aluminum that is formed after dehydration at T > 110 °C and which is seen in Al K edge XANES.[25] This change in coordination has not been monitored by $^{27}$Al MAS NMR spectroscopy, since in dehydrated samples the quadrupolar interaction increases, thus reducing appreciably the resolution of the spectra.[17]

The proposed scheme takes into account the 1:1 ratio between the proton species corresponding to the framework Al(OH) sites and the octahedral aluminum species, as reported.[23] The number of proton species associated with framework AlOH sites was estimated using $^{1}$H MAS NMR spectroscopy after degassing at 110 °C, thus when the aluminum is in the tetrahedral state (b). The number of octahedral aluminum species was determined by $^{27}$Al MAS NMR spectroscopy in wet conditions, thus when the aluminum is in the octahedral state (a).

In general, it should be taken into consideration that in the dehydrated state the octahedral aluminum is converted into tetrahedral, and that the techniques that are applied in a dehydrated state, like $^{1}$H MAS NMR or FTIR spectroscopy, probe the presence of species (b). This is different from techniques that are applied in a hydrated state, which probe species (a).

Species (c) is formed after dehydration following adsorption of a base and has been observed by both $^{27}$Al MAS NMR and FTIR spectroscopy.

**4.3. Nature of EFAl Species in Zeolite USY.** $^{27}$Al (MQ) MAS NMR spectroscopy showed the presence of at least three different octahedral species in zeolite H−USY (Figure 1). Both 6-coordinated species $Al(VI)_a$ and $Al(VI)_c$ adopted tetrahedral coordination after ammonia adsorption, indicating the presence of reversible species in zeolite H−USY (Figures 1 and 2). They can either be associated with zeolitic framework aluminum species or, as was discussed above, with aluminum atoms belonging to an amorphous silica−alumina phase. Surely they cannot be present in alumina debris, since this material did not show any change in coordination upon ammonia adsorption (Figure 5). The $Al(VI)_a$ species experiences a quadrupolar interaction of 2 MHz, corresponding to the values found in pure zeolitic materials (Table 4). Therefore it is attributed to reversible aluminum associated with the zeolite framework. $Al(VI)_c$ shows a large distribution in chemical and quadrupolar shift. The $C_{QCC}$ value for $Al(VI)_c$ is 3.8 MHz, and corresponds to the values found for the octahedral aluminum species in amorphous silica−alumina (Table 4). Therefore it is assigned to nonframework aluminum associated with an amorphous silica−alumina phase formed during the ultrastabilization process. Transition aluminas have been proposed as a model for the nonframework aluminum in zeolite USY.[29] From a comparison of the distributions and quadrupolar and chemical shift parameters, Fyfe et al. later reported that amorphous alumina gel is not a good model for the extraframework aluminum species in USY.[12] The formation of amorphous alumino−silicates was previously proposed for dealuminated zeolite Y.[8] Kellberg et al. also evidenced analogies between the nonframework aluminum phase in zeolite H−USY and amorphous silica−alumina. The two materials showed the same change in the $^{27}$Al MAS NMR spectrum upon acetylacetone treatment.[9] The peak at 32 ppm in zeolite USY was assigned to tetrahedrally coordinated species belonging to amorphous silica−alumina.[11] $^{1}$H MAS NMR spectroscopy showed similarities between the proton species in dealuminated zeolites Y and amorphous silica−alumina as a function of dehydration−rehydration treatments.[13] As discussed in ref 30, amorphous silica−alumina forms from the reaction between the extracted silicon and aluminum in the postsynthesis solution. In the specific case under study, probably alumina domains are present in amorphous silica−alumina, as suggested by the presence of residual octahedral species in zeolite H−USY after saturation with gaseous ammonia (Figures 1 and 2). However, these species could be associated with aluminum species positioned in extraframework octahedral sites as well, as described in ref 7. The amount of such species is rather high in zeolite H−USY (Table 2). This is not surprising, since the formation of silica−alumina is favored by the dissolution of silicon during the steaming process. If the amount of silicon in solution is low, the formation of alumina domains and/or charged octahedral species will obviously be favored.

## 5. Conclusions

The aluminum coordination of different alumino−silicate materials was studied by means of $^{27}$Al (MQ) MAS NMR spectroscopy. Upon ammonia adsorption at 120 °C, a conversion from octahedral to tetrahedral coordination was observed for zeolites and amorphous silica−alumina, showing that the reversibility of the aluminum coordination is a general feature of alumino−silicate systems. The distinction between zeolitic material and amorphous silica−alumina is possible, based on the $C_{QCC}$ values of the octahedrally coordinated species. For silica−alumina, the conversion was only partial and the extent of the conversion was an inverse function of the aluminum content. The fraction of aluminum species whose coordination was unaffected by ammonia adsorption is probably associated with alumina domains. This agrees with the fact that the aluminum coordination in $\gamma$-$Al_2O_3$ was not affected by the same treatment. A distinction between pure alumino−silicate material and alumina domains in amorphous silica−alumina was therefore possible. A considerable amount of aluminum atoms in zeolite H−USY changed their coordination from octahedral to tetrahedral upon ammonia adsorption. Most of these are aluminum atoms belonging to amorphous silica−alumina formed during the ultrastabilization treatment. A small fraction is represented by framework zeolitic aluminum.

**Acknowledgment.** The authors thank Prof. B. Meyer for providing the measuring time at the Bruker Avance DSX-600 NMR spectrometer and Dr. A. Detken for helping during the measurements. Dr. Jaap N. Louwen (AKZO Nobel Catalysts) is acknowledged for discussion on the octahedral structure.

## References and Notes

(1) Beyerlein, R. A.; ChoiFeng, C.; Hall, J. B.; Huggins, B. J.; Ray, G. J. *Top. Catal.* **1997**, *4*, 27.

(2) Klinowski, J.; Thomas, J. M.; Fyfe, C. A.; Gobbi, G. C. *Nature* **1982**, *296*, 533.

(3) Klinowski, J.; Fyfe, C. A.; Gobbi, G. C. *J. Chem. Soc., Faraday Trans. I* **1985**, *81*, 3003.

(4) Freude, D.; Brunner, E.; Pfeifer, H.; Prager, D.; Jerschkewitz, H. G.; Lohse, U.; Oehlmann, G. *Chem. Phys. Lett.* **1987**, *139*, 325.

(5) Blumenfeld, A. L.; Fripiat, J. J. *Top. Catal.* **1997**, *4*, 119.

(6) Remy, M. J.; Stanica, D.; Poncelet, G.; Feijen, E. J. P.; Grobet, P. J.; Martens, J. A.; Jacobs, P. A. *J. Phys. Chem.* **1996**, *100*, 12440.

(7) van Bokhoven, J. A.; Roest, A. L.; Koningsberger, D. C.; Miller, J. T.; Nachtegaal, G. H.; Kentgens, A. P. M. *J. Phys. Chem. B* **2000**, *104*, 6743.

(8) Sanz, J.; Fornes, V.; Corma, A. *J. Chem. Soc., Faraday Trans. I* **1988**, *84*, 3113.

(9) Kellberg, L.; Linsten, M.; Jakobsen, H. J. *Chem. Phys. Lett.* **1991**, *182*, 120.

(10) Janin, A.; Maache, M.; Lavalley, J. C.; Joly, J. F.; Raatz, F.; Szydlowski, N. *Zeolites* **1991**, *11*, 391.

(11) Menezes, S. M. C.; Camorim, V. L.; Lam, Y. L.; San Gil, R. A. S.; Bailly, A.; Amoureux, J. P. *Appl. Catal., A—General* **2001**, *207*, 367.

(12) Fyfe, C. A.; Bretherton, J. L.; Lam, L. Y. *J. Am. Chem. Soc.* **2001**, *123*, 5285.

(13) Dorémieux-Morin, C.; Martin, C.; Brégeault, J. M.; Fraissard, J. *Appl. Catal.* **1991**, *77*, 149.

(14) Kato, Y.; Shimizu, K.; Matsushita, N.; Yoshida, T.; Yoshida, H.; Satsuma, A.; Hattori, T. *Phys. Chem. Chem. Phys.* **2001**, *3*, 1925.

(15) Frydman, L.; Harwood: J. S. *J. Am. Chem. Soc.* **1995**, *117*, 5367.

(16) Medek, A.; Harwood: J. S.; Frydman, L. *J. Am. Chem. Soc.* **1995**, *117*, 12779.

(17) Kentgens, A. P. M. *Geoderma* **1997**, *80*, 271.

(18) Müller, M.; Harvey, G.; Prins, R. *Microporous Mesoporous Mater.* **2000**, *34*, 281.

(19) Amoureux, J. P.; Fernandez, C.; Steuernagel, S. *J. Magn. Reson. Ser. A* **1996**, *123*, 116.

(20) Ernst, R.; Bodenhausen G.; Wokaun, A. *Principles of Nuclear Magnetic Resonance in One and Two Dimensions*; Oxford University Press: New York, 1987.

(21) Bourgeat-Lami, E.; Massiani, P.; Di Renzo, F.; Espiau, P.; Fajula, F.; Courieres, T. D. *Appl. Catal.* **1991**, *72*, 139.

(22) van Bokhoven, J. A.; Koningsberger, D. C.; Kunkeler, P.; van Bekkum, H.; Kentgens, A. P. M. *J. Am. Chem. Soc.* **2000**, *122*, 12842.

(23) Wouters, B. H.; Chen, T. H.; Grobet, P. J. *J. Am. Chem. Soc.* **1998**, *120*, 11419.

(24) Woolery, G. L.; Kuehl, G. H.; Timken, H. C.; Chester, A. W.; Vartuli, J. C. *Zeolites* **1997**, *19*, 288.

(25) van Bokhoven, J. A.; van der Eerden A. M. J.; Koningsberger, D. C. *Stud. Surf. Sci. Catal.* **2002**, *142*, 1885.

(26) Hitz, S.; Prins, R. *J. Catal.* **1997**, *168*, 194.

(27) Basila, M. R.; Kantner, T. R. *J. Phys. Chem.* **1967**, *71*, 467.

(28) Trombetta, M.; Busca, G.; Rossini, S.; Piccoli, V.; Cornaro, U.; Guercio, A.; Catani, R.; Willey, R. J. *J. Catal.* **1998**, *179*, 581.

(29) Coster, D.; Blumenfeld, A. L.; Fripiat, J. J. *J. Phys. Chem.* **1994**, *98*, 6201.

(30) Omegna, A.; Haouas, M.; Kogelbauer, A.; Prins, R. *Microporous Mesoporous Mater.* **2001**, *46*, 177.